Research Article Vol. 2, No. 2 / 15 Feb 2023 / Optics Continuum 498
OPTICS CONTINUUM

Dysprosium gain-switched fiber laser at 3.24 µm pumped at 1064 nm

FRÉDÉRIC JOBIN,* YIĞIT OZAN AYDIN, MARTIN BERNIER, AND RÉAL VALLÉE

Centre d'optique, photonique et laser (COPL), Université Laval, Québec City, Québec G1V 0A6, Canada
**frederic.jobin.3@ulaval.ca*

Abstract: We report a dysprosium-doped gain switched fluoride fiber laser pumped at 1064 nm and emitting at 3244 nm. Pulses with energies up to 1 µJ were generated on a wide range of repetition rates between 100 kHz and 200 kHz, the highest reported for a pulsed dysprosium-doped fiber laser, producing an average output power reaching 207 mW. Stable 8.9 µJ pulses were also generated near 10 kHz, which is the highest pulse energy reported to date from a 1.1 µm band pumped dysprosium-doped fiber laser. This shows the 1.1 µm band as a valuable alternative for the pumping of dysprosium-doped fiber lasers emitting far from the emission peak and is thus of potential interest for future field applications.

1. Introduction

Lasers emitting in the wavelength range extending from 3 µm to 3.5 µm have seen significant progress in recent years due to their high potential for numerous applications [1]. While lasers emitting around 3 µm are of great interest for biomedical applications [2] due to the presence of water absorption bands, applications in the fields of hydrocarbon remote sensing would benefit from sources emitting between 3.2 µm and 3.4 µm [3,4] while polymer processing could use sources could use sources emitting from 3.25 µm to 3.55 µm [5,6]. Dual-wavelength pumped erbium-doped fiber lasers have been previously studied, but their emission was mainly limited to the 3.4 µm-3.5 µm band [7–9], and thus leaving a gap between 3 µm and 3.4 µm. Dysprosium, while its transition is ground terminated, is a promising candidate due to its wide emission cross-section to provide laser sources covering this range and addressing the requirements for environmental and industrial applications.

Fluoride based dysprosium-doped fiber lasers have been demonstrated as early as 2003 [10], but it is only in the past six years that significant progress was achieved for this class of lasers. While the dysprosium ion exhibits numerous absorption bands as illustrated in Fig. 1, most demonstrations have been focused on those around 1.1 µm and 2.8 µm due to the availability of powerful pumping sources at these wavelengths through Yb^{3+}:SiO_2 and Er^{3+}:ZBLAN fiber lasers, respectively. In a continuous wave regime, the 2.8 µm pumping scheme has produced the most significant results, allowing Watt-level emission with 73% efficiency [11], a 91% slope efficiency [12] and a 10 W-level laser at 3.24 µm [13]. Recently, 3 W of output power were achieved at 3.42 µm [14], showing the potential of dysprosium-doped fiber lasers for industrial applications. Dysprosium lasers using a 1.1 µm pumping wavelength have shown more limited performances, producing up to 554 mW of output power [15] and a 23% slope efficiency [16], which is quite respectable considering the high quantum defect of the pumping scheme. The 1.7 µm pumping band of the dysprosium ion, while lacking readily available laser sources, was used to achieve a wide tuning range of 700 nm [17].

Pulsed dysprosium-doped fiber lasers have also seen significant progress in recent years although there have been few demonstrations reported. Mode-locking of this laser transition was first demonstrated using frequency-shifted feedback producing 33 ps pulses with a maximum of 2.7 nJ at 44.5 MHz [18]. Nonlinear polarisation evolution allowed to produce pulses as short

#480593 https://doi.org/10.1364/OPTCON.480593
Journal © 2023 Received 10 Nov 2022; revised 23 Jan 2023; accepted 24 Jan 2023; published 15 Feb 2023

OPTICS CONTINUUM

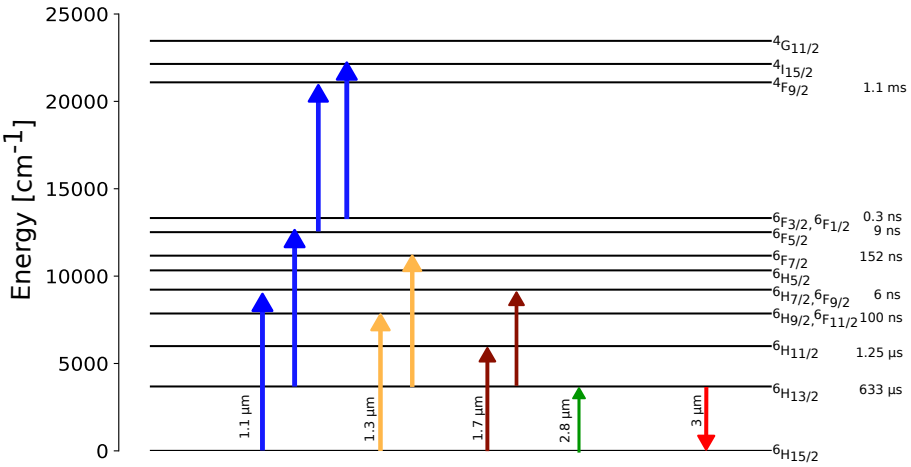

Fig. 1. Simplified energy diagram of the dysprosium ion in a fluoride glass matrix

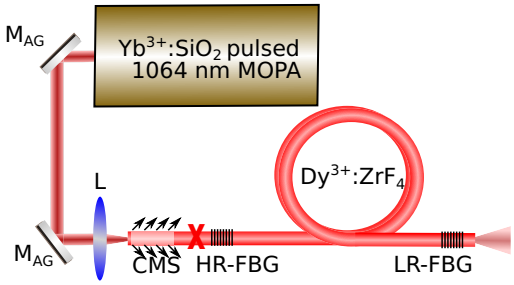

Fig. 2. Experimental setup of the dysprosium-doped gain-switched fiber laser. M_{Ag}, silver mirror; L, lens; CMS, cladding mode stripper; HR-FBG, high-reflectivity fiber Bragg grating; LR-FBG, low-reflectivity fiber Bragg grating.

as 828 fs with 4.8 nJ energy at 60 MHz [19]. *Q*-switched was demonstrated both in the active and passive regime [20–23]. These lasers have been mostly focused on emission at the peak of the $^6H_{13/2} \rightarrow {}^6H_{15/2}$ transition near 2.95 µm with some demonstrations offering tunability from 2.74 µm to 3.34 µm [23]. The highest energy achieved was of 12 µJ for an actively *Q*-switched fiber laser pumped at 2.8 µm [20], while the other demonstrations produced energies under 2 µJ. All these demonstrations produced pulses in the 250–800 ns range for repetition rates ranging from 0.1-170 kHz.

Very few gain-switched dysprosium-doped fiber lasers have been demonstrated until now. Using a 1.1 µm pump, up to 4.36 µJ of pulse energy was achieved for a repetition rate of 80 kHz with a laser tunable from 2.8 µm to 3.1 µm [24]. Gain-switching near the emission peak of dysprosium at 2.94 µm was also demonstrated using a 1.1 µm pump, producing 0.72 µJ of pulse energy for a repetition rate of 50 kHz [25]. The in-band 2.8 µm pumping scheme has produced the highest pulse energy and average power yet with 19.3 µJ pulses and an average power up to 1.4 W with a laser operating from 20 kHz to 120 kHz at a wavelength of 3.24 µm [26].

In this paper, we report the demonstration of a dysprosium-doped gain-switched fiber laser emitting at 3.24 µm using a 1064 nm pulsed pumped system. The laser produced stable microsecond pulses from 100 kHz to 200 kHz and at 10 kHz, with the operating limits inherent to the pumping source. A maximum pulse energy of 8.9 µJ was achieved at 10 kHz, which is the

OPTICS CONTINUUM

highest reported from a dysprosium-doped pulsed fiber laser pumped in the 1.1 µm band. At higher repetition rates, the pulse energy was limited to 1.04 µJ. This work is thus extending the wavelength coverage of 1.1 µm pumped dysprosium doped-fiber lasers as well as their repetition rate range.

2. Experimental setup

Figure 2 illustrates the experimental setup of the gain-switched cavity, which was made of a 1.06 m long dysprosium-doped fluoride fiber segment bounded by two fiber Bragg gratings written in the active fiber. The fiber, manufactured by *Le Verre Fluoré*, had a 16 µm/250 µm geometry with a NA of 0.12 and a doping concentration of 2000 ppm, providing an estimated absorption of approximately 20 dB/m at 1064 nm. The fiber Bragg gratings were both written through the coating using the phase mask technique [27–30]. The input HR-FBG had a reflectivity of 95% near 3244 nm with a FWHM of less than 0.4 nm. It was written in a damage-free type-I regime to minimize losses at 1064 nm since core pumping was used. The LR-FBG had a reflectivity of 55% and a FWHM of 1.6 nm. It was written in a type-II (damage) regime, as a relatively high reflectivity over a wide range was required to ensure overlap with the HR-FBG and to minimize the laser threshold.

A 1064 nm pumping wavelength was chosen as laser systems operating in this wavelength range are well understood, high power systems can be achieved and the use of a silica fiber-based pumping system is attractive for practical reasons compared to the in-band 2.8 µm band where fluoride fibers are required. The 3.24 µm cavity was pumped by a homemade Yb^{3+}:SiO_2 three-stage pulsed MOPA system which was free space coupled. This system allowed operation from 10 kHz to 200 kHz with adjustable pulses from 30 ns to 500 ns and average power reaching up to 10 W at high repetition rates. Due to the onset of parasitic amplified spontaneous emission (ASE) in the MOPA system, its average power and thus pulse energy were limited as the repetition rate was reduced with an average output power of around 2.8 W at 10 kHz. The multimode nature of the output beam, the mode mismatch, and the requirement for core-pumping produced a modest injection efficiency of 37%, which was measured using a mode matched passive fiber. A cladding mode stripper (CMS) consisting of a $\approx$ 10 cm length of stripped fiber re-coated with high index polymer was applied at the fiber input to reduce the thermal load on the tip caused by the pump signal injected in the fiber cladding that was coated with a high-index polymer.

Both pump and signal pulse trains were measured simultaneously with fast photodiodes (Alphalas UPD-5N-IR2-P for the 1064 nm signal and Thorlabs PDAVJ8 for the 3.24 µm signal) and a 10 GHz oscilloscope (Agilent DSO81004A). The average power was measured by a Gentec thermal detector (XLP12-3S-H2-D0) and the laser spectrum by an optical spectrum analyser (Yokogawa AQ6375L). All measurements were done simultaneously using filters to remove any residual pump and no parasitic wavelengths were observed while monitoring the spectrum on a wide band.

3. Results

The dysprosium doped gain-switched fiber laser had an emission band centered at 3244.5 nm with a 3 dB bandwidth of 0.2 nm as illustrated in Fig. 3. The laser spectrum was fixed by the narrow HR-FBG and no significant wavelength shift was observed throughout operation. Due to the core-pumping scheme of the cavity and the type-II nature of the LR-FBG, residual pump could not be measured, although the relatively low temperature elevation of the LR-FBG indicated little 1064 nm signal was passing through, as residual pump scattered by the FBG would have led to a significant temperature increase during operation. The temperature was monitored using a Jenoptik thermal camera and all components showed a low thermal load under passive cooling provided by a copper fiber groove.

OPTICS CONTINUUM

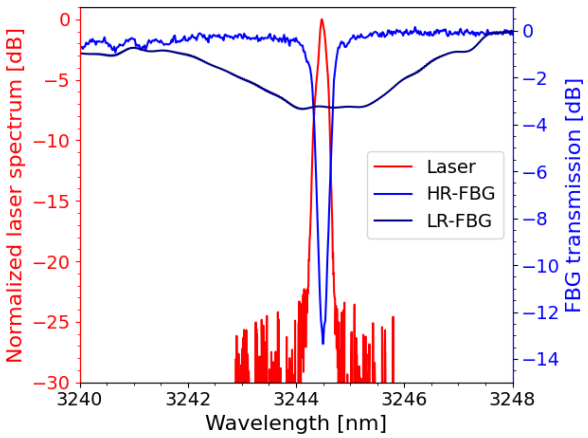

Fig. 3. Fiber Bragg grating transmission spectra and gain-switched laser emission spectrum.

The laser average output power was measured as a function of launched pump power for the repetition rates which spanned the stable pulsed regime of the system. As illustrated in Fig. 4, the measured slope efficiency was consistently around 10% for all repetition rates and the laser threshold was around 1.5 W of launched pump power. A slight increase of laser power at the threshold can be observed as a function of the repetition rate, indicating an increase in overall efficiency for faster repetition rates. This is likely explained by the relatively short 640 µs lifetime of the $^6H^{13/2}$ level of dysprosium, leading to the decay of some ions to the ground level, and reducing the average population as the repetition rate decreases. The large quantum defect between the pump and signal wavelengths limits the achievable efficiency to around 33%. Another factor limiting the overall efficiency is the relatively high reflectivity (i.e. 55%) of the LR-FBG, purposely made stronger than the optimum value of around 40% in order to minimize the laser threshold and maximize the operation range for a wide span of repetition rates. Optimum cavity parameters were estimated based on preliminary numerical simulations.

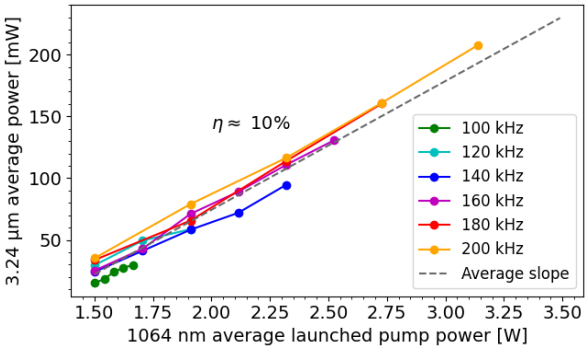

Fig. 4. Average output power of the dysprosium-doped fiber laser as a function of launched pump power for various repetition rates.

The laser pulses were characterized as a function of pump pulse energy and repetition rate, as illustrated in Fig. 5. Stable pulses could be achieved near 10 kHz and from 100 kHz to 200 kHz. The limitations in terms of repetition rates were caused by the 1064 nm pumping system. As a matter of fact, the achievable pulse energy was limited at repetition rates below 100 kHz due to the onset of parasitic ASE which could lead to a catastrophic failure of the system through the

OPTICS CONTINUUM

generation of giant pulses in the Yb^{3+} amplifier stages. Between 10 kHz and 100 kHz, pulses were observed at the output of the dysprosium-doped fiber laser. However the pump pulse energy was not sufficient to achieve a stable dynamic in which one pump pulse led to one signal pulse in a repeatable manner.

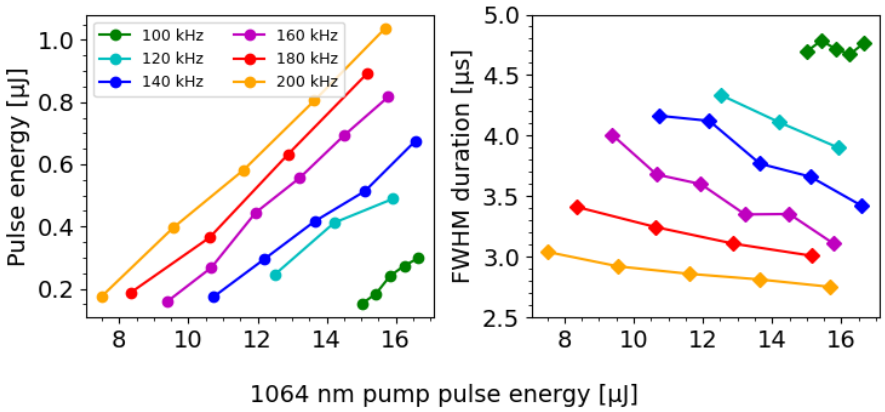

Fig. 5. 3.24 µm pulse energy (left) and duration (right) as a function of pump pulse energy for repetition rates ranging from 100 kHz to 200 kHz.

At a repetition rate of 10 kHz (this single point is not illustrated to avoid skewing the figures), pulses with an energy of 8.9 µJ were generated, corresponding to an average power of 89 mW, which is the highest pulse energy achieved with a dysprosium-doped pulsed fiber laser pumped around 1.1 µm, while also being at a wavelength far from the emission peak of the ion. At this repetition rate, the operation range of the laser was very limited, as a launched pump power below 1.5 W did not allow the generation of stable pulses and higher pump powers could not be achieved without risking a failure of the pumping system due to parasitic ASE. Between 100 kHz and 200 kHz, a wider operation range could be achieved, however, producing lower pulse energies, ranging from 0.2 µJ to 1 µJ. These pulses had a full width at half-maximum (FWHM) ranging from 3 µs to 5 µs, significantly longer than the pump pulses. The peak powers achieved were very modest, being less than a watt, owing to the long pulse duration. The pumping system used, being based on a passively *Q*-switched oscillator, the pulse energy decreased as a function of the repetition rate. However, faster repetition rates, allowed a greater pumping of the amplification stages, thus mitigating this effect to a certain extent.

The pump and signal pulse trains are illustrated in Fig. 6 for repetition rates of 10 kHz and 100 kHz, and illustrate the stability of the pulses. The pulse exhibited fast substructures corresponding to a cavity round-trip duration (~11 ns). However these substructures were highly unstable from one pulse to the next. This can be explained by the high resonance of the cavity with very reflective FBGs and the presence of multiple longitudinal modes as previously observed in gain-switched fiber lasers [31,32]. Although these fast fluctuations vary significantly, the pulse envelope was stable. Pulse envelope RMS variations were of around 9% at 10 kHz and reduced to around 4.3% at 100 kHz and 3.4% at 200 kHz. These variations could not be correlated to the very weak pulse to pulse fluctuations of the pump. It should, however, be noted that the stability of the signal pulses increased with the pumping energy until the onset of second signal pulse, caused by excess pump energy. At 10 kHz, the observed pulses were close to the lower bound of the stable emission range due to power limitations imposed by the Yb^{3+} pumping system.

Figure 7 illustrates a pump and signal pulse, at a repetition rate of 10 kHz and 100 kHz. At all repetition rates, the pump pulses were significantly shorter than the signal pulses and had a correspondingly higher peak power. The pump pulses were in the 30 ns–500 ns range, while the

OPTICS CONTINUUM

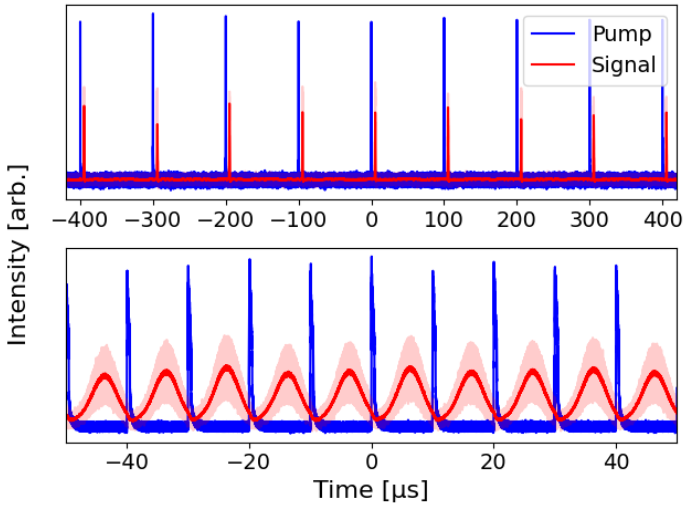

Fig. 6. Pump and signal pulse trains at 10 kHz (top) and 100 kHz (bottom). The pale red curve illustrates the fast fluctuations, while the dark red one indicates the pulse envelope

envelope of the signal pulses varied between 3 µs and 5 µs. As both pulse trains were measured simultaneously, the delay between the pump and signal pulses corresponds to the cavity build-up time.

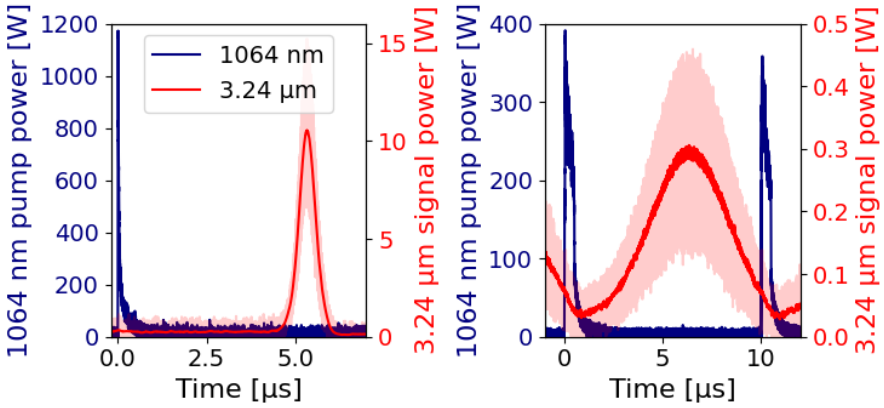

Fig. 7. Pump and signal pulse shape at a repetition rate of 10 kHz (left) and 100 kHz (right). The pale red curve illustrates the fast fluctuations, while the dark red one indicates the pulse envelope

While some cavity parameters such as high FBG reflectivity and potential immeasurable losses in the active fiber or output coupler, are sure to affect the pulse duration, the laser dynamics involved in this system are clearly in play. These long pulses in turn limit the maximum repetition rate achievable. As it can be seen in Fig. 7, at 100 kHz, the pulses cover the time span between two pump pulses, and at faster repetition rates, the second pump pulse steepens the drop of the pulse envelope's trailing edge. The pulses while long are more or less of similar duration than those reported in previous demonstrations by other groups [20,21,24]. This can be explained by the relatively low pulse energy (below 20 µJ) and long duration (500 ns) of the pump pulses compared to our previous demonstration with in-band pumping [26]. It is also likely that 1064 nm pumping

OPTICS CONTINUUM

slows the dynamics of the laser compared to in-band pumping due to the number of levels involved and their underlying dynamics. Several excited state absorption and energy transfer mechanisms [33,34] are sure to influence time-dependent dynamics. Numerical simulations will likely lead to a better understanding of the these laser dynamics, however they are not easily achievable at the current time due to a lack of knowledge of the spectroscopic parameters involved, especially regarding the various excited-state absorptions (ESAs) and potential energy transfers [33,35].

While the pumping of dysprosium-doped fiber lasers with Yb^{3+} systems presents some challenges such as a lower quantum efficiency than in-band pumping, this approach has its merits. One should note that several operating limitations were caused by the pumping source, and not the Dy^{3+}-doped laser. Since Yb^{3+}:SiO_2 fiber lasers are much more technologically mature than their Er_{3+}:ZrF_4 counterparts, the design of an optimized pumping source is much more likely using this pumping scheme.

4. Conclusion

We have demonstrated the operation of a 3.24 µm gain-switched fiber laser pumped at 1064 nm, achieving pulses up to 8.9 µJ at 10 kHz and also producing stable pulses on a wide range of repetition rates from 100 kHz to 200 kHz. These results represent the highest energy from a 1.1 µm band pump dysprosium pulsed fiber laser and the widest range of repetition rates for such lasers while being at an operation wavelength significantly far from the emission peak and of great interest for potential field applications such as remote methane sensing and material processing. The average slope efficiency achieved was a respectable 10%, and varied very little between repetition rates. A maximum output power of 207 mW was produced at 200 kHz.

Further investigations should consider the optimization of the pump pulse shapes and duration as it has been done in theory for in-band pumping [36], but will likely be easier to achieve around 1.1 µm. Furthermore, the development of silica to fluoride glass splices [37] will allow the development of entirely monolithic systems, achieving the ruggedness required for field applications.

Funding. Fonds de recherche du Québec – Nature et technologies (144 616, CO256655); Canada Foundation for Innovation (5180); Natural Sciences and Engineering Research Council of Canada (IRCPJ469414-13, RGPIN-2016-05877).

Acknowledgments. The authors would like to thank Pascal Paradis for helpful discussions and Sébastien Magnan-Saucier for technical assistance.

Disclosures. The authors declare no conflicts of interest.

Data availability. Data underlying the results presented in this paper are not publicly available at this time but may be obtained from the authors upon reasonable request.

References

1. F. Jobin, P. Paradis, Y. O. Aydin, T. Boilard, V. Fortin, J.-C. Gauthier, M. Lemieux-Tanguay, S. Magnan-Saucier, L.-C. Michaud, S. Mondor, L.-P. Pleau, L. Talbot, M. Bernier, and R. Vallée, "Recent developments in lanthanide-doped mid-infrared fluoride fiber lasers," Opt. Express **30**(6), 8615–8640 (2022).
2. M. C. Pierce, S. D. Jackson, M. R. Dickinson, T. A. King, and P. Sloan, "Laser-tissue interaction with a continuous wave 3-µm fibre laser: preliminary studies with soft tissue," Lasers Surg. Med. **26**(5), 491–495 (2000).
3. B. M. Walsh, H. R. Lee, and N. P. Barnes, "Mid infrared lasers for remote sensing applications," J. Lumin. **169**, 400–405 (2016).
4. M. F. S. Ferreira, E. Castro-Camus, D. J. Ottaway, J. M. López-Higuera, X. Feng, W. Jin, Y. Jeong, N. Picqué, L. Tong, B. M. Reinhard, P. M. Pellegrino, A. Méndez, M. Diem, F. Vollmer, and Q. Quan, "Roadmap on optical sensors," J. Opt. **19**(8), 083001 (2017).
5. C. Frayssinous, V. Fortin, J. P. Bérubé, A. Fraser, and R. Vallée, "Resonant polymer ablation using a compact 3.44 µm fiber laser," J. Mater. Process. Technol. **252**, 813–820 (2018).
6. M. R. Majewski, G. Bharathan, A. Fuerbach, and S. D. Jackson, "Long wavelength operation of a dysprosium fiber laser for polymer processing," Opt. Lett. **46**(3), 600–603 (2021).
7. O. Henderson-Sapir, J. Munch, and D. J. Ottaway, "Mid-infrared fiber lasers at and beyond 3.5 µm using dual-wavelength pumping," Opt. Lett. **39**(3), 493–496 (2014).

OPTICS CONTINUUM

8. M. Lemieux-Tanguay, V. Fortin, T. Boilard, P. Paradis, F. Maes, L. Talbot, R. Vallée, and M. Bernier, "15 W monolithic fiber laser at 3.55 μm," Opt. Lett. **47**(2), 289–292 (2022).
9. O. Henderson-Sapir, J. Munch, and D. J. Ottaway, "Wavelength Tunable mid-infrared Er^{3+}:ZBLAN fiber laser at 3.5 μm using dual wavelength pumping," in *CLEO: 2015*, (OSA, Washington, D.C., 2015), p. SW1L.5.
10. S. D. Jackson, "Continuous wave 2.9 μm dysprosium-doped fluoride fiber laser," Appl. Phys. Lett. **83**(7), 1316–1318 (2003).
11. R. I. Woodward, M. R. Majewski, G. Bharathan, D. D. Hudson, A. Fuerbach, and S. D. Jackson, "Watt-level dysprosium fiber laser at 3.15 μm with 73% slope efficiency," Opt. Lett. **43**(7), 1471–1474 (2018).
12. M. R. Majewski, M. Z. Amin, T. Berthelot, and S. D. Jackson, "Directly diode-pumped mid-infrared dysprosium fiber laser," Opt. Lett. **44**(22), 5549 (2019).
13. V. Fortin, F. Jobin, M. Larose, M. Bernier, and R. Vallée, "10-W-level monolithic dysprosium-doped fiber laser at 3.24 μm," Opt. Lett. **44**(3), 491–494 (2019).
14. L.-P. Pleau, V. Fortin, and T. Boilard, "Long wavelength multi-watt dysprosium fiber laser for resonant polymer ablation," Advanced Solid State Lasers **2021**, 4–5 (2021).
15. L. Sojka, L. Pajewski, M. Popenda, E. Beres-Pawlik, S. Lamrini, K. Markowski, T. Osuch, T. M. Benson, A. B. Seddon, and S. Sujecki, "Experimental investigation of mid-infrared laser action from Dy^{3+} doped fluorozirconate fiber," IEEE Photonics Technol. Lett. **30**(12), 1083–1086 (2018).
16. Y. H. Tsang and A. E. El-taher, "Efficient lasing at near 3 μm by a Dy-doped ZBLAN fiber laser pumped at 1.1 μm by an Yb fiber laser," Laser Phys. Lett. **8**(11), 818–822 (2011).
17. Y. Wang, H. Luo, H. Gong, H. Wu, Y. Lyu, J. Li, and Y. Liu, "Watt-level and tunable operations of 3 μm-class dysprosium ZrF_4 fiber laser pumped at 1.69 μm," IEEE Photonics Technol. Lett. **34**(14), 737–740 (2022).
18. R. I. Woodward, M. R. Majewski, and S. D. Jackson, "Versatile mid-infrared mode-locked fiber laser, electronically tunable from 2.97 to 3.30 μm," in *CLEO Pacific Rim:2018*, (2018), p. PDP.8.
19. Y. Wang, F. Jobin, S. Duval, V. Fortin, P. Laporta, M. Bernier, G. Galzerano, and R. Vallée, "Ultrafast Dy^{3+} :fluoride fiber laser beyond 3 μm," Opt. Lett. **44**(2), 395 (2019).
20. R. I. Woodward, M. R. Majewski, N. Macadam, G. Hu, T. Albrow-Owen, T. Hasan, and S. D. Jackson, "Q-switched Dy:ZBLAN fiber lasers beyond 3 μm: comparison of pulse generation using acousto-optic modulation and inkjet-printed black phosphorus," Opt. Express **27**(10), 15032–15045 (2019).
21. H. Luo, J. Li, Y. Gao, Y. Xu, X. Li, and Y. Liu, "Tunable passively Q-switched Dy^{3+} -doped fiber laser from 2.71 to 3.08 μm using PbS nanoparticles," Opt. Lett. **44**(9), 2322–2325 (2019).
22. Y. Wang, T. T. Fernandez, P. Tang, N. Coluccelli, S. D. Jackson, M. C. Falconi, F. Prudenzano, P. Laporta, and G. Galzerano, "Mid-IR tunable CW and passively Q-switched laser operation of Dy-doped fluoride fiber," Opt. Mater. Express **12**(4), 1502 (2022).
23. Y. Wang, H. Luo, H. Wu, J. Li, and Y. Liu, "Tunable pulsed dysprosium laser within a continuous range of 545 nm around 3 μm," J. Lightwave Technol. **40**(14), 4841–4847 (2022).
24. H. Luo, Y. Xu, J. Li, and Y. Liu, "Gain-switched dysprosium fiber laser tunable from 2.8 to 3.1 μm," Opt. Express **27**(19), 27151–27158 (2019).
25. L. Pajewski, L. Sójka, S. Lamrini, T. M. Benson, A. B. Seddon, and S. Sujecki, "Gain-switched Dy^{3+} :ZBLAN fiber laser operating around 3 μm," J. Phys. Photonics **2**(1), 014003 (2020).
26. F. Jobin, P. Paradis, V. Fortin, S. Magnan-Saucier, M. Bernier, and R. Vallée, "1.4 W in-band pumped Dy^{3+} -doped gain-switched fiber laser at 3.24 μm," Opt. Lett. **45**(18), 5028–5031 (2020).
27. R. Vallée, M. Bernier, and D. Faucher, "System and method for permanently writing a diffraction grating in a low phonon energy glass medium," (2011).
28. J. Habel, T. Boilard, J. S. Frenière, F. Trépanier, and M. Bernier, "Femtosecond FBG written through the coating for sensing applications," Sensors **17**(11), 2519 (2017).
29. M. Bernier, R. Vallée, F. Trépanier, and J. Carrier, "Writing of high mechanical strength fiber Bragg gratings using ultrafast pulses and a phase mask," US Patent 10,845,533 (2020).
30. S. Jackson, R. Vallée, and M. Bernier, eds., *Mid-Infrared Fiber Photonics* (Elsevier, 2021), 1st ed.
31. C. Larsen, K. P. Hansen, K. E. Mattsson, and O. Bang, "The all-fiber cladding-pumped Yb-doped gain-switched laser," Opt. Express **22**(2), 1490–1499 (2014).
32. P. Paradis, V. Fortin, Y. O. Aydin, R. Vallée, and M. Bernier, "10 W-level gain-switched all-fiber laser at 2.8 μm," Opt. Lett. **43**(13), 3196–3199 (2018).
33. L. Gomes, A. F. H. Librantz, and S. D. Jackson, "Energy level decay and excited state absorption processes in dysprosium-doped fluoride glass," J. Appl. Phys. **107**(5), 053103 (2010).
34. A. G. Okhrimchuk, A. D. Pryamikov, K. N. Boldyrev, L. N. Butvina, and E. Sorokin, "Collective phenomena in Dy-doped silver halides in the near- and mid-IR," Opt. Mater. Express **10**(11), 2834–2848 (2020).
35. S. D. Jackson and M. R. Majewski, "Role of energy transfer in concentrated Dy^{3+} -doped fibers," OSA Continuum **4**(10), 2591 (2021).
36. M. C. Falconi, D. Laneve, M. Bozzetti, T. T. Fernandez, G. Galzerano, and F. Prudenzano, "Design of an efficient pulsed Dy^{3+}: ZBLAN fiber laser operating in gain switching regime," J. Lightwave Technol. **36**(23), 5327–5333 (2018).
37. S. Cozic, S. Boivinet, C. Pierre, J. Boulet, S. Poulain, and M. Poulain, "Splicing fluoride glass and silica optical fibers," in *EPJ Web of Conferences*, vol. 215 O. Fähnle and A. Vasdekis, eds. (2019), p. 04003.